Chapter 11

Quantum information and many-body systems

This final chapter is devoted to an application of basic quantum information theory concepts in the context of strongly correlated systems and, more in general, of condensed matter physics. Recent groundbreaking experiments in the spirit of Feynman's idea of quantum simulators enabled to manipulate certain quantum many-body systems in a very accurate and controlled way, thus paving the way for a tremendously increasing theoretical activity in this field. We will see that a closer look to the intimate entanglement structure of typical many-body wave functions may reveal itself extremely helpful to understand the physics of such systems. Indeed, on this basis, it has been possible to conceive powerful analytical and numerical methods to uniquely characterize the thermodynamical properties of a wide class of complex quantum systems.

After glimpsing at how non-trivial quantum frustration mechanisms may emerge in such context, we shall consider in detail the spin-1/2 quantum Ising chain, and thoroughly present its analytic solution. This paradigmatic example of quantum many-body system provides a convenient playground where it is possible to recognize the emergence of a very peculiar behaviour for the ground-state entanglement, far from being specific to a single model. The latter observation can be formalized through the concept of the area-law scaling of bipartite quantum correlations for the low-energy states of generic locally interacting strongly correlated systems.

The second part of the chapter is devoted to an introduction of the so-called tensor-network formalism for quantum many-body lattice systems, a tool that is able to provide a reliable Ansatz for any wave function satisfying certain entanglement constraints in the Hilbert space. Emphasis is put on the simplest case of one-dimensional systems, where the so-called matrix product states (MPS) naturally emerge as a consequence of the area-law requirement for the bipartite entanglement. We shall discuss the density-matrix renormalization group algorithm, a variational technique for finding the ground state over the MPS class of wave functions. We also show how to manipulate such states to study real-time evolution, finite-temperature states, and systems coupled to an external environment. Finally we briefly focus on tensor-network schemes for higher dimensions, and on hierarchical structures which may violate the area-law constraint.

11.1 Quantum simulators

Understanding the thermodynamic behaviour of many-body quantum systems is a formidable task which tantalized the attention of many generations of physicists, starting from the dawn of quantum mechanics. This observation is particularly urgent in the context of non-equilibrium dynamics. Unfortunately up to a decade ago, even conceiving any experiment of controlled dynamics at the nanoscale was mostly seen as a chimera, due to the extreme difficulty in tailoring and controlling the physical setup. For this reason, the problem covered a purely academic interest.

The advent of the so-called *quantum simulators* profoundly changed this scenario: they enabled to realize a new concept of quantum devices originally devised by Feynman (1982), which could "mimic the physics of other quantum systems". Such devices have unveiled the possibility to operate in the lab at the level of the single quantum object, with an exceptionally low degree of decoherence and high tunability. It is now possible to carefully probe the interplay between dimensionality, interactions and quantum coherence in a wealth of different physical implementations, from Josephson-junction arrays, to ultracold quantum gases, semiconductor nanostructures, and coupled quantum electrodynamical (QED) cavities. In some cases one may even engineer the dissipation in a controlled way, as a resource to probe the behaviour of driven-dissipative systems.

In synthesis, quantum simulators are fabricated devices that can experimentally simulate the model Hamiltonian underlying the non-trivial properties of the physical systems under consideration. The advantages of this approach are twofold. First of all, it is possible to explore the properties of strongly correlated model Hamiltonians also in the regions of the phase diagram which are elusive to numerical and analytical investigations. Secondly, it allows to test to which extent the model Hamiltonians are appropriate to treat the physical systems that they are supposed to describe, or whether additional ingredients are necessary.

11.1.1 *Ultracold atoms*

The first nano fabricated devices, designed with the specific purpose to simulate the physics of strongly correlated systems, were probably Josephson-junction arrays. The field however acquired full maturity only with the appearance of cold atoms trapped in magneto-optical potentials, which proved to be excellent simulators of a large variety of strongly interacting Fermi and Bose systems. The success of these latter systems, virtually immune to disorder, relies on their ultra-small coupling to the environment and to the extremely low operating temperatures, of the order of few nano Kelvin. This allows to access the equilibrium, as well as the non-equilibrium dynamics of closed many-body systems (a regime lying outside the experimental capabilities with more traditional solid-state systems).

As a matter of fact, cold atoms can be manipulated with an unprecedented accuracy. First of all, it is possible to trap them in periodic potentials that are

generated by shining two counter-propagating laser beams, which may interfere to form a modulated optical standing wave, the so-called *optical lattices*. Such artificial crystals, almost free from defects and vibrations, can be loaded with thousands of neutral atoms obeying either Bose or Fermi statistics (or even mixtures of them), such that each site may contain only few particles, of the order of one. Moreover, a good control over the collision properties of atoms can be achieved by tuning external parameters across the so-called Feshbach resonances [1], making it possible to increase the two-body interaction strength and access a deep quantum regime of strongly correlated particles.

As shown by Jaksch *et al.* (1998), the prototype non-trivial Hamiltonian that can be naturally simulated by means of ultracold bosonic atoms loaded in an optical lattice is the *Bose–Hubbard model*. This is given by

$$H \;=\; -J \sum_{\langle i,j \rangle} \left(b_i^\dagger b_j + \text{H.c.} \right) + \frac{U}{2} \sum_j n_j (n_j - 1), \tag{11.1}$$

where the indices i and j label the various minima of the optical standing wave (i.e., the sites of the artificially constructed lattice), and the brackets $\langle \cdot, \cdot \rangle$ limit the summation to nearest-neighbour pairs of sites. In the second quantization language, the operators $b_j^{(\dagger)}$ annihilate (create) a boson on the j-th site of the lattice ($n_j = b_j^\dagger b_j$ is the corresponding number operator, which counts how many bosons are located on the j-th site). We postpone a more rigorous theoretical analysis of such class of systems to Sec. 11.2.1, while providing here only a qualitative discussion in order to grasp its salient physical features.

The low-temperature physics of the Bose–Hubbard model is dominated by the competition between delocalization, induced by the hopping of bosons between adjacent cavities (the first term in Eq. (11.1), with strength $J > 0$), and on-site repulsive interaction (the second term in Eq. (11.1), with strength $U > 0$). Specifically, the ground state phase diagram consists of two phases. If the hopping term dominates over the interaction, that is $J \gg U$, the system enters a *superfluid* (SF) state where each atom tends to be spread over all the lattice, and the corresponding many-body wave function is a product of delocalized single-particle states:

$$|\psi\rangle_{\text{SF}} \;\propto\; \left(\sum_{j=1}^{L} b_j^\dagger \right)^N |0\rangle \,, \tag{11.2}$$

where N is the total number of bosons in a lattice of L sites, and $|0\rangle$ is the vacuum of particles. The characteristic feature of this state is that of representing a macroscopic wave function, which possesses long-range phase coherence throughout the lattice. In the opposite limit where interactions dominate, that is $U \gg J$, the

[1] A Feshbach resonance describes the resonant scattering between two particles, when their incoming energies are very close to those of a two-particle bound state. It is possible to control their energy difference either via a magnetic field, or by optical methods. As a result of this process, the scattering length of the two atoms can be modified, thus providing a way to vary the interaction strength between atoms in the cloud by changing scattering length of elastic collisions. For a recent review, see Chin *et al.* (2010).

fluctuations in the atomic number on each site are very small, and the system stabilizes into a sequence of localized atomic wave functions with a fixed number of atoms per lattice site. In the case of a commensurate filling of $n = N/L$ atoms per site, the global wave function can be written as a product of Fock states:

$$|\psi\rangle_{\rm MI} \propto \prod_{j=1}^{L} \left(b_j^\dagger\right)^n |0\rangle \,, \tag{11.3}$$

whose resulting many-body features are that of a so-called *Mott insulator* (MI). This latter state does not entail phase coherence, and cannot be described by a macroscopic wave function.

In their seminal paper, Fisher *et al.* (1989) theoretically showed that, for integer values of n, a zero-temperature phase transition between the above mentioned SF and MI phases takes place at a finite value of the U/J ratio. On the other hand, for non-integer fillings the bosons are always superfluid. Thirteen years later, this transition was experimentally observed by Greiner *et al.* (2002): In response to a change in the relative strength of U vs. J (as obtained by tuning the optical lattice depth, through a control of the intensity of the trapping lasers), two clearly distinct types of matter wave interference pattern were spotlighted. Specifically, Fig. 11.1 displays experimentally observed absorption images of matter waves; the various panels from **(a)** to **(h)** stand for increasing values of U/J. As is clearly visible, in the SF phase interference fringes can be observed [panels **(a)-(f)**] while in the MI phase they completely disappear [panels **(g)-(h)**].

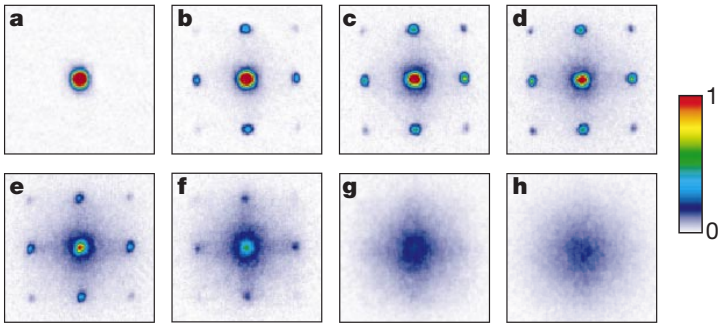

Fig. 11.1 Interference patterns of matter waves as obtained after releasing a confining three-dimensional optical lattice, and measuring the absorption of atoms on a screen at a fixed distance from the initial lattice. The various panels correspond to different optical potential depths, which tune the relative strength of U/J in Eq. (11.1). The figure is reprinted with permission from Greiner *et al.* (2002). ©(2002) Macmillan Magazines Ltd.

The extreme versatility of cold atoms also enables them to probe quantum magnetism through the direct measure of quantum correlations, thus opening up the possibility to study strongly correlated states of matter at very low temperatures. As an example, we quote the simulation of two-component fermionic models by Greif

et al. (2013), where nearest neighbour spin-spin correlations have been measured by means of cooling schemes based on the local redistribution of entropy within the lattice structure (see Fig. 11.2).

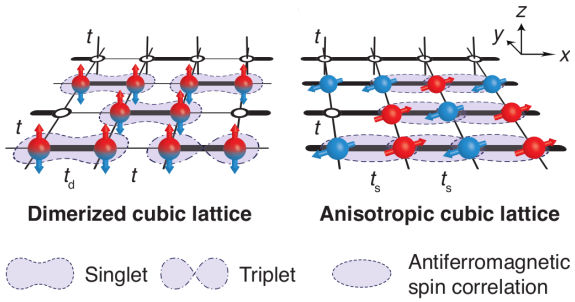

Fig. 11.2 Sketch of the magnetic spin-spin correlations that have been measured with a two-component ultracold Fermi gas with repulsive interactions, loaded in a three dimensional cubic lattice. The system may be found into either a dimerized or an anisotropic configuration, depending on the relative strength of the tunnel terms along each spatial dimension. Drawing courtesy of Tilman Esslinger, Zurich.

However ultracold atoms are not the only available quantum simulators. As already discussed in Sec. 10.2.1, within the field of atomic and molecular optics, it is also possible to build up highly controllable systems of up to few tens of heavier ions, which can be trapped in electromagnetic potentials. In a completely different scenario, one could devise ensembles of QED cavities that are coupled together, such as to form artificial lattice structures.

11.1.2 *Arrays of coupled QED cavities*

A cavity array consists of a regular arrangement of QED cavities which, in the original conception, can be coupled through a photon-hopping mechanism. The emerging physical scenario is basically dominated by the interplay of two effects: on the one hand, light-matter interaction inside each cavity may lead to a strong effective Kerr nonlinearity between photons; on the other hand, photon hopping between neighbouring cavities favours delocalization, thus competing with the photon nonlinearity. The idea of implementing many-body states with light has been originally proposed in this context by Greentree *et al.* (2006), Hartmann *et al.* (2006) and Angelakis *et al.* (2007), showing that coupled cavities could be taken as another possibility towards the realization of quantum simulators.

Despite their young age, as compared to the more mature field of ultracold atoms in optical lattices or of ion-trap experiments, cavity arrays present a valid alternative to realize strongly correlated states of light. Indeed they can operate at high temperatures (with respect to Josephson arrays and optical lattices), and allow for single-site addressing, opening a clear way to experimentally access the

correlation functions. Most importantly, cavity arrays are specifically designed to be open-system quantum simulators, thus representing an opportunity to explore the physics of many-body quantum systems in contact with an environment. They naturally operate under non-equilibrium conditions: the population of photons that leak out because of unavoidable losses should be refilled by an external drive. Two classes of problems can be addressed: On the one hand, they offer a valid platform to understand how to realize and detect, under realistic non-equilibrium conditions, the dynamical counterpart of equilibrium phases for the underlying strongly-interacting models (Bose–Hubbard model, interacting spin models, ...), in situations where a steady state is formed. On the other hand, they pave the way to study the emerging non-equilibrium phase diagram in a controlled scenario, a field which is still, to a large extent, an unexplored territory. This may lead, as well, to the stabilization of exotic ordering, driven by completely new cooperative mechanisms.

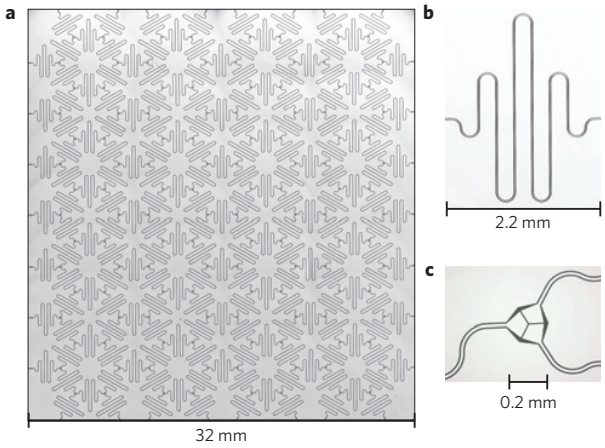

Fig. 11.3 QED cavities can be coupled in a lattice for quantum simulation. This figure shows a superconducting circuit of more than two hundred 7 GHz microwave cavities, coupled in a two dimensional Kagome lattice structure. The junction between neighbouring cavities is realized by coupling capacitors, which enable photon hopping. Interactions between photons can be provided by adding superconducting qubits (an example is the so-called Cooper-pair box, constituted by two superconducting islands connected by two Josephson junctions, forming a superconducting quantum interference device) to the cavities, using an additional lithography layer. The figure is reprinted with permission from Houck *et al*. (2012). ©(2012) Macmillan Publishers Ltd.

There are several possible platforms that may lead to the implementation of a cavity array. One could engineer a photonic crystal, by coupling quantum dots to photonic band gap defect nanocavities. Another possibility are silicon structures of either a disc or a toroidal shape, where the light is trapped in whispering gallery modes that are localized close to the outer surface of the structure and have a small mode volume. We also mention Fabry-Pérot cavities where photons can be coupled

into and from each cavity through optical fibers, or using suitable on-chip arrays of cavity micro-mirrors. The most promising platform however seems to be based on present-day circuit-QED technology, through the use of superconducting resonators and Josephson junctions: scalable arrays of hundreds of cavities in large mesoscopic structures at the millimeter scale have been already realized (see Fig. 11.3).

Theoretical model of a cavity array

As discussed above, the simplest Hamiltonian which describes an array of coupled cavities must include the light-matter interaction within each cavity, and the coupling between different (in many cases only neighbouring) cavities:

$$H = \sum_i H_i^{(\text{cavity})} + \sum_{\langle i,j \rangle} H_{i,j}^{(\text{coupl})} , \tag{11.4}$$

where the indices i and j label the position of a cavity on a generic d-dimensional lattice structure. The first term takes into account the dynamics of an isolated cavity, while the second one describes the interaction between cavities.

As explained in Sec 10.1.2, the minimal model of a cavity QED is the so-called Jaynes–Cummings Hamiltonian H_{JC} of Eq. (10.7). In the strong-coupling regime, light-matter interaction turns the cavity into a turnstile device, where only a photon can be present at the same time. Intuitively, this can be understood as the fact that one photon in the cavity strongly modifies the effective resonance frequency, inhibiting the injection of a second photon. This phenomenon has been termed *photon blockade*, after the Coulomb blockade effect of electrons in mesoscopic structures (see Imamōglu *et al.*, 1997). In several situations, as in circuit-QED, counter-rotating terms cannot be neglected, leading to the Rabi Hamiltonian H_{Rabi} of Eq. (7.111).

The coupling between cavities can have different origin, depending on the implementation. In the simplest scenario, if the cavities are sufficiently close to allow for photon hopping, an additional kinetic term

$$H_{i,j}^{(\text{coupl})} = -J\big(a_i^\dagger a_j + \text{H.c.}\big) \tag{11.5}$$

describes the tunnelling of a photon from the i-th to the j-th cavity, with an associated J rate. The operator $a_j^{(\dagger)}$ annihilates (creates) a photon in the mode of the j-th cavity. In certain implementations it is even possible to couple two cavities through non-linear elements, such that $H_{i,j}^{(\text{coupl})}$ would also contain cross-Kerr interaction terms, and/or correlated hopping terms.

The Hamiltonian in Eq. (11.4) bears strong similarities with the Bose–Hubbard model of Eq (11.1), and for this reason, it is sometimes referred to as the *Jaynes–Cummings–Hubbard model*. The similarity is evident: instead of the local on-site repulsion controlled by U, the non-linearity in the spectrum of Jaynes-Cummings–Hubbard model appears because of the light-matter interaction. Nonetheless, the competition between delocalization and local non-linearity does not crucially depend on these detailed differences.

Any realistic description of cavity arrays cannot exclude losses. In cavity systems there are numerous sources of dissipation and decoherence that need to be taken

into account, such as decoherence and relaxation of the atoms inside the cavities, and photon losses. In most relevant cases the latter are the dominant contribution, therefore here we only consider these ones. In the presence of losses, the state of the array can be faithfully described by its density matrix ρ, which obeys the GKLS master equation (7.169). Assuming that each cavity is coupled to an independent environment, the action of the dissipation can be modeled by the Lindblad operators

$$L_j \,=\, \sqrt{\kappa}\, a_j \tag{11.6}$$

on each cavity, with κ being the inverse of the photon lifetime. The fixed point of the resulting master equation is the vacuum state: eventually all the photons will have escaped from the cavities and the atoms will have decayed in their ground state. In order to refill the array with photons, an external drive is needed. If the pump is coherent it will contribute to an extra term in the Hamiltonian of the form

$$H_{\rm drive} \,=\, \Omega \sum_j \big(a_j^\dagger + a_j\big). \tag{11.7}$$

The driving can be either continuous, or time-modulated through a laser pulse sequence. In the first case the array reaches a steady state, as a result of the interplay of the coherent and incoherent contributions to the dynamics of ρ; in the latter case an initial population imbalance is formed, which subsequently relaxes to the vacuum state. More in general, a wealth of peculiar phenomena associated to non-equilibrium phases and phase transitions have been recently shown to emerge in such systems, as experimentally realized in Fitzpatrick *et al*. (2017). For a detailed discussion, we refer the interested reader to the literature in the bibliography.

D-Wave device

In the last ten years, a scalable implementation of a circuit-QED quantum simulator has been realized by the private Canadian company D-Wave Systems Inc., with the intent to develop the first commercial "quantum computer" (see: `http://www.dwavesys.com`). This eventually led to the commercialization, starting from 2011, of prototype devices ranging from 128 (D-Wave One) to 2048 coupled qubits (D-Wave 2000Q), which have been purchased by big companies as, for example, Lockheed Martin, Google, and NASA.

The building block of the hardware is a so-called superconducting quantum interference device (SQUID), namely, a very sensitive magnetometer based on a superconducting loop containing Josephson junctions. The interference refers to the fact that different magnetic spin states (typically encoded in clockwise and anti-clockwise circulating current in the loop), which constitute the two levels of one qubit, can be put into a quantum mechanical superposition. In order to go from a single qubit to a multi-qubit processor, the qubits are then coupled by means of superconducting circuits. Here we will not detail the implementation of such device, but only briefly discuss its working principle.

As a matter of fact, D-Wave is not a device that implements quantum gates: it is an adiabatic quantum computer for solving optimization problems, in the spirit

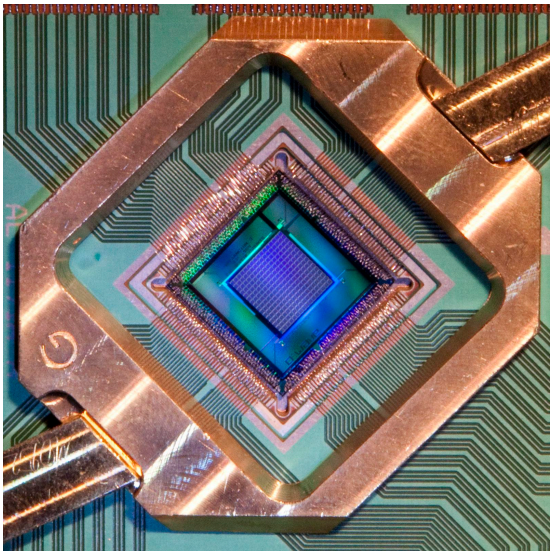

Fig. 11.4 Photograph of the D-Wave 2000Q chip, manufactured by D-Wave Systems Inc.

of what has been discussed in Sec. 3.13. Namely, the superconducting qubits are initialized into their lowest energy state, then suitable magnetic fields are gently modulated in time, in such a way as to drive this state (pseudo-)adiabatically toward a new one. This process is usually referred to as *quantum annealing*, and a machine like D-Wave is a *quantum annealer.*. The possibility to realize this protocol with systems made of many qubits is particularly significant, since any quantum algorithm of arbitrary difficulty can be formulated in terms of identifying the global minimum (the ground state $|\psi_F\rangle$) of a given function (the Hamiltonian H_F) over a set of many local minima [2]. Provided the annealing protocol can be performed in a limited amount of time, in principle this would represent an exponential speedup with respect to any classical computation. It should be however stressed that, posing a problem in a form that D-Wave can handle, often requires several qubits to represent a single variable, thus limiting the size of the treatable problems.

Among the quantum annealing protocols, a particularly relevant one is the crossing of a quantum phase transition, an occurrence which typically emerges for any hard problems encoded in the annealer. If the control parameter is slowly changed on a timescale much larger than the typical inverse zero-temperature gap, the sys-

[2]More precisely, Barahona (1982) has formally shown that finding the ground state of disordered spin-glass models of the Ising type in arbitrary geometry (similar to the classical version of the Ising model discussed in Sec. 11.3) belongs to the class of NP-complete classical problems. Unfortunately, it is presently not known whether there exists an efficient quantum algorithm, belonging to the BQP class, which would be able to solve such NP-complete problems in an efficient way (see Sec. 1.3.2 for a brief discussion on the complexity classes).

tem stays in its instantaneous ground state, unless a critical point is crossed. In the latter case, the system is unable to follow the driving and to remain in its equilibrium/ground state: a finite density of defects will be produced, thus invalidating the outcome of the simulation. The problem of defect formation in the adiabatic dynamics of critical systems was examined well before quantum information, by Kibble (1976) and Zurek (1985), in the context of phase transitions in the early universe, and later extended to the quantum case, giving rise to an intense discussion (see, for example, Dziarmaga (2010)). The Kibble-Zurek mechanism roughly divides the dynamics in either adiabatic or impulsive, according to the distance from the critical point. The time at which the system switches from one regime to another depends on the annealing speed: the slower it is, the later the evolution will become impulsive. This allows to predict the scaling of such defects as a function of the rate of the annealing procedure, in terms of the critical exponents of the crossed phase transition.

The picture outlined above sheds light on the intrinsic limitations of the quantum annealing approach: the solution to "hard" problems, encoded into the ground state of H_F, cannot be adiabatically connected, through a time-dependent protocol of the type in Eq. (3.182), with the ground state $|\psi_0\rangle$ an "easy" Hamiltonian H_I. More precisely, for NP problems the connection $H(t)$ requires the passage through a critical point, where the gap closes exponentially with the system size, thus requiring an exponentially large amount of time for the annealing process to reach the target state $|\psi_F\rangle$. Moreover, as explained before, the presence of the coupling with the external environment for this kind of cavity-QED devices inevitably leads to decoherence. This represents a highly detrimental effect for the annealer. Nonetheless some preliminary studies, as the ones of Johnson *et al.* (2011), Boixo *et al.* (2013), and Lanting *et al.* (2014), have shown that genuine quantum effects, including the presence of entanglement, can survive in D-Wave machines already with few tens of qubits. Evidence of the power of quantum annealing was spotlighted even with more than one hundred coupled qubits (Boixo *et al.*, 2014). However, whether these machines already hold the so-called "quantum advantage" or not (that is, a clear exponential speedup over classical computers), is still under fervid debate (see, for example, Rønnow *et al.*, 2014, and Boixo *et al.*, 2018).

11.2 Emergence of quantum correlations

We now characterize more in detail some prototypical many-body systems on a lattice, whose physics can be naturally addressed by means of the quantum simulators described in the previous section. Specifically, here we would like to provide a flavour of how genuine quantum frustration effects may emerge, as a result of two or more competing mechanisms.

11.2.1 *The Hubbard model*

The Hubbard model is perhaps the simplest representative model of interacting quantum particles on a lattice, describing localized electronic orbitals, with on-site repulsive interactions between particles on the same site (Hubbard, 1963). To a good approximation it mimics what occurs in a crystal at low temperatures and in the Born-Oppenheimer approximation: few valence electrons per atom move in a periodic potential, in the lowest Bloch band, ignoring any long-range interactions between the electrons. The motion of electrons can be separated from that of nuclei, whose positions are supposed to be fixed in space, thus defining the underlying lattice structure. The Hamiltonian can be written as:

$$H = -t \sum_{\langle i,j\rangle,\sigma} (c^\dagger_{i,\sigma} c_{j,\sigma} + \text{H.c.}) + U \sum_j n_{j,\uparrow} n_{j,\downarrow} \,, \tag{11.8}$$

where $c^{(\dagger)}_{i,\sigma}$ denote annihilation (creation) operators for electrons with a given spin $\sigma = \uparrow, \downarrow$, on the i-th site of the lattice. These satisfy the anti-commutation relations $\{c_{i,\sigma}, c^\dagger_{j,\tau}\} = \delta_{ij}\,\delta_{\sigma\tau}$ and $\{c_{i,\sigma}, c_{j,\tau}\} = \{c^\dagger_{i,\sigma}, c^\dagger_{j,\tau}\} = 0$, where δ_{ij} is the Kronecker symbol [3]. The first term in Eq. (11.8), with coupling constant $t > 0$, accounts for the possibility of an electron with spin σ to hop from the i-th site to an adjacent j-th site of the lattice. The interaction term, with strength $U > 0$, acts on states in which there are two particles on a given site (i.e., one particle of each spin state on the same site, since the Pauli principle prevents double occupancy of the same site with the same spin state), thus making them energetically unfavoured. The emerging scenario is similar to that discussed in Sec. (11.1.1), albeit with particles obeying a different quantum statistics.

In typical situations, the electrons are tightly bounded to the nuclei of the atoms, so that the interaction strength is much larger than the hopping amplitude: $U \gg t$. Moreover let us focus on the case of one electron per site, so that the number of electrons and the number of lattice sites will match. If interactions were absent, the Hubbard model would simply describe a conductor: the band is indeed half filled with one electron per site (thus there is no doping), but with two possible spin states per site. Due to translational invariance, for $U = 0$ the model can be diagonalized straightforwardly in momentum space, with a sinusoidal dispersion relation in the momentum k. Conversely, in the presence of strong interactions the system becomes insulating, as it costs an energy $U \gg t$ to move an electron onto an already singly occupied site.

Mapping to effective spin models

We now concentrate on the magnetic properties of the insulating phase, and perform a second-order perturbation theory in the hopping term of Eq. (11.8), that is, we

[3] The particles in Eq. (11.8) need not to be necessarily fermions, as in Hubbard's original work. One could also consider bosonic particles $b^{(\dagger)}_i$ satisfying the commutation relations $[b_i, b^\dagger_j] = \delta_{ij}$; $[b_i, b_j] = [b^\dagger_i, b^\dagger_j] = 0$. This gives rise to the Bose–Hubbard model of Eq. (11.1).

write $H = H_0 + \delta H$, where H_0 is the interaction term (U) and the perturbation δH is the hopping term (t). We start by considering a pair of sites, hosting two electrons at half filling, and compare the energies of the triplet/singlet states:

$$|1,1\rangle = |\uparrow,\uparrow\rangle, \quad |1,0\rangle = \tfrac{1}{\sqrt{2}}\big(|\uparrow,\downarrow\rangle + |\downarrow,\uparrow\rangle\big), \quad |1,-1\rangle = |\downarrow,\downarrow\rangle, \tag{11.9}$$

$$|0,0\rangle = \tfrac{1}{\sqrt{2}}\big(|\uparrow,\downarrow\rangle - |\downarrow,\uparrow\rangle\big). \tag{11.10}$$

Since all these states have the same occupation on each site, and the hopping term will produce something orthogonal to each state, it is clear that at leading order:

$$\langle 1,1|\delta H|1,1\rangle = \langle 1,0|\delta H|1,0\rangle = \langle 1,-1|\delta H|1,-1\rangle = \langle 0,0|\delta H|0,0\rangle = 0. \tag{11.11}$$

However at second order in the hopping, the energy correction to the eigenstates $|n\rangle$ of H_0 is no longer zero, indeed:

$$\delta E_n^{(2)} = \sum_{m\neq n} \frac{\langle n|\delta H|m\rangle\langle m|\delta H|n\rangle}{E_n^{(0)} - E_m^{(0)}}, \tag{11.12}$$

where $|m\rangle$ are intermediate virtual states which admit double occupancy on a single site, while $E_n^{(0)}$ is the zero-th order energy of $|n\rangle$.

It is immediate to see that $\delta H|1,1\rangle = \delta H|1,-1\rangle = 0$, since, due to Pauli principle, the hopping cannot move a spin up (down) particle to a site already occupied by a spin up (down) particle. For the other two states $\delta H|1,0\rangle$ and $\delta H|0,0\rangle$, we need to fix a sign convention determined by the ordering of fermionic operators. We adopt the following choice: from left to right (i) operators appear in the same order as sites, and (ii) spin-up operators appear first. For example: $|\uparrow\downarrow,\downarrow\rangle = c^\dagger_{1,\uparrow}c^\dagger_{1,\downarrow}c^\dagger_{2,\downarrow}|\Omega\rangle$, where $|\Omega\rangle$ is the vacuum state. Therefore we have:

$$\begin{aligned}\delta H|\uparrow,\downarrow\rangle &= -t\big(c^\dagger_{1,\uparrow}c_{2,\uparrow} + c^\dagger_{2,\uparrow}c_{1,\uparrow} + c^\dagger_{1,\downarrow}c_{2,\downarrow} + c^\dagger_{2,\downarrow}c_{1,\downarrow}\big)c^\dagger_{1,\uparrow}c^\dagger_{2,\downarrow}|\Omega\rangle \qquad (11.13)\\ &= -t\big(c^\dagger_{2,\uparrow}c_{1,\uparrow}c^\dagger_{1,\uparrow}c^\dagger_{2,\downarrow} + c^\dagger_{1,\downarrow}c_{2,\downarrow}c^\dagger_{1,\uparrow}c^\dagger_{2,\downarrow}\big)|\Omega\rangle = -t(c^\dagger_{2,\uparrow}c^\dagger_{2,\downarrow} + c^\dagger_{1,\uparrow}c^\dagger_{1,\downarrow})|\Omega\rangle\\ \delta H|\downarrow,\uparrow\rangle &= -t\big(c^\dagger_{1,\uparrow}c_{2,\uparrow} + c^\dagger_{2,\uparrow}c_{1,\uparrow} + c^\dagger_{1,\downarrow}c_{2,\downarrow} + c^\dagger_{2,\downarrow}c_{1,\downarrow}\big)c^\dagger_{1,\downarrow}c^\dagger_{2,\uparrow}|\Omega\rangle \qquad (11.14)\\ &= -t\big(c^\dagger_{1,\uparrow}c_{2,\uparrow}c^\dagger_{1,\downarrow}c^\dagger_{2,\uparrow} + c^\dagger_{2,\downarrow}c_{1,\downarrow}c^\dagger_{1,\downarrow}c^\dagger_{2,\uparrow}\big)|\Omega\rangle = t(c^\dagger_{1,\uparrow}c^\dagger_{1,\downarrow} + c^\dagger_{2,\uparrow}c^\dagger_{2,\downarrow})|\Omega\rangle,\end{aligned}$$

where we used the fermionic ordering introduced above, and (in the last equalities of the two above expressions) the anti-commutation relations. It is thus clear that

$$\delta H|1,0\rangle = 0, \quad \delta H|0,0\rangle = -\frac{2t}{\sqrt{2}}\big(|\uparrow\downarrow,0\rangle + |0,\uparrow\downarrow\rangle\big), \tag{11.15}$$

so that the singlet state is energetically favoured, with

$$\delta E^{(2)}_{0,0} = \frac{2t\times 2t}{0-U} = -\frac{4t^2}{U}. \tag{11.16}$$

We have thus discovered that, at second order in perturbation theory for $U \gg t$, there is an antiferromagnetic interaction of strength $J = 4t^2/U$, which favours the projection onto the singlet state. Coming back to the pair of spin-1/2 particles, we can consider the operator

$$\mathbf{S}_1\cdot\mathbf{S}_2 = \frac{1}{2}\Big[\big(\mathbf{S}_1+\mathbf{S}_2\big)^2 - \mathbf{S}_1^2 - \mathbf{S}_2^2\Big] = \begin{cases} \frac{1}{2}\big(0 - 2\times\frac{3}{4}\big) = -\frac{3}{4} & \text{for a singlet,}\\ \frac{1}{2}\big(2 - 2\times\frac{3}{4}\big) = +\frac{1}{4} & \text{for a triplet,}\end{cases} \tag{11.17}$$

where $\mathbf{S}_j = \boldsymbol{\sigma}_j/2$ and $\boldsymbol{\sigma}_j = (\sigma_j^x, \sigma_j^y, \sigma_j^z)$ are the usual Pauli matrices on the j-site. In this way, the effective hopping term can be written as an isotropic magnetic interaction of the form $J\,(\mathbf{S}_1 \cdot \mathbf{S}_2)$, with $J = 4t^2/U$. In the many-body scenario of several pairs of spin-1/2 particles, this leads to the following effective Hamiltonian:

$$H_{\text{eff}} \sim -J \sum_{\langle i,j \rangle} \mathcal{P}_{\text{singlet}}(i,j) = \frac{4t^2}{U} \sum_{\langle i,j \rangle} \mathbf{S}_i \cdot \mathbf{S}_j, \tag{11.18}$$

where, according to Eq. (11.17), $\mathcal{P}_{\text{singlet}}(i,j) = \frac{1}{4} - \mathbf{S}_i \cdot \mathbf{S}_j$ is the projector on the singlet state. This is named the antiferromagnetic spin-1/2 *Heisenberg model*.

At this point it is crucial to observe that, when considering a lattice of more than two sites (with a spin-1/2 particle per site), H_{eff} would prefer to place all the neighbouring spins in a singlet state. This is however not possible, and a problem of *quantum frustration* arises. Indeed, since the singlet state $|0,0\rangle$ of Eq. (11.10) forms a maximally entangled Bell pair, the discussion in Sec. (6.8.1) tells us that, for any two spins A and B that are placed in such configuration, the monogamy of entanglement forbids to create any quantum state where the pair would be entangled with any other spin C. Specifically if A and B are in a singlet state, the concurrence $C_{AB} = 1$; then Eq. (6.103) implies that $C_{AC} = 0$, and thus A cannot be entangled with C. This simple argument exemplifies the possibility to establish a highly non-trivial pattern of quantum correlations in complex many-body systems, clearly hinting at the fact that perturbative methods around a single state (as a pure state or Bloch waves) typically do not work in the presence of strong interactions.

In the remainder of this chapter, we will first discuss the prototypical example of an exactly solvable quantum many-body system. Later we will address a wider scenario, where general considerations on the scaling of bipartite entanglement for the low-lying energy states of a class of Hamiltonian models enable us to develop a theory that well captures the low-energy physics of typical strongly correlated quantum systems.

11.3 The spin-1/2 quantum Ising chain

In this section we present the one-dimensional (1D) quantum Ising chain in a transverse magnetic field, for spin-1/2 particles. This covers a pivotal importance for the understanding of the statistical mechanics of 1D quantum many-body systems. The possibility to find an easy analytical solution, firstly devised by Lieb *et al.* (1961) and by Pfeuty (1970), makes it the ideal playground where several emerging pivotal aspects of strongly correlated systems can be discussed. The Hamiltonian is

$$H = -J \sum_j \sigma_j^x \sigma_{j+1}^x - h \sum_j \sigma_j^z\,, \tag{11.19}$$

where the spin-1/2 Pauli matrices σ_j^α ($\alpha = x, y, z$) are defined on each site j of the chain ($j = 1, \ldots, L$ with L being the chain length), J denotes the nearest-neighbour coupling and h the magnetic field strength. For the sake of clarity and without loss of generality, we assume an antiferromagnetic coupling $J > 0$.

We are going to show how it is possible to fully diagonalize Eq. (11.19) using a Jordan–Wigner transformation into a quadratic fermionic Hamiltonian, followed by a Bogoliubov rotation in momentum space. We first concentrate on basic properties of the ground state, like its energy, magnetization and spin-spin correlation functions. These results, as well as a series of additional analytical findings on the whole excitation spectrum in out-of-equilibrium conditions which will not be touched in this presentation, can be found in a series of seminal papers by Barouch, McCoy and coworkers (Barouch *et al.*, 1970; Barouch and McCoy, 1971a,b; McCoy *et al.*, 1971). Later we will discuss more recent results where ground-state correlations have been reinterpreted in a quantum-information context, unveiling a peculiar behaviour for specific entanglement measures. Finally we will describe how the Ising chain can be read in the context of Majorana physics.

Let us first transform the spin-1/2 particles into hard-core bosons a_j, by identifying $|\downarrow\rangle \leftrightarrow |0\rangle$ and $|\uparrow\rangle \leftrightarrow |1\rangle$ at each site. The operators $a_j^{(\dagger)}$ commute at different sites (as the original Pauli operators do), but are not ordinary bosonic operators, because they must satisfy the hard-core constraint $\left(a_j^\dagger\right)^2 |0\rangle = 0$, that is, at most one boson per site is allowed. Using the definition of the raising and lowering spin operators $\sigma_\pm = \frac{1}{2}(\sigma_x \pm i\sigma_y)$, which act as $\sigma_+|\downarrow\rangle = |\uparrow\rangle$, $\sigma_-|\uparrow\rangle = |\downarrow\rangle$, we get:

$$\sigma_j^+ = a_j^\dagger, \quad \sigma_j^- = a_j, \quad \sigma_j^z = 2a_j^\dagger a_j - 1\,. \tag{11.20}$$

Notice that on the same site $\{\sigma_j^-, \sigma_j^+\} = 1$, thus implying that $\{a_j, a_j^\dagger\} = 1$, while ordinary bosons would have the commutator. In terms of hard-core bosons, the Ising Hamiltonian of Eq. (11.19) becomes:

$$H = -J \sum_j \left(a_j^\dagger a_{j+1} + a_j^\dagger a_{j+1}^\dagger + \text{H.c.}\right) - h \sum_j (2a_j^\dagger a_j - 1). \tag{11.21}$$

The next step is to switch to ordinary fermionic operators, with which it is possible to easily diagonalize the model.

11.3.1 *Jordan–Wigner transformation*

The hard-core constraint introduced above for the bosonic operators a_j seems to be ideally representable in terms of spinless fermions, where the absence of double occupancy is automatically enforced by the Pauli exclusion principle, and the anti-commutation on the same site comes for free. Unfortunately, since fermion operators on different sites anti-commute (while the bosons a_j commute), the resulting minus sign must be correctly handled by performing a non-local mapping, which is called the *Jordan–Wigner transformation* (JWT). Specifically, the JWT of hard-core a_j bosons into c_j fermions reads:

$$a_j = K_j c_j = e^{i\pi \sum_{i<j} n_i} c_j = \left[\prod_{i=1}^{j-1} (1 - 2n_i)\right] c_j, \tag{11.22}$$

where $n_j = c_j^\dagger c_j$ is the fermion number operator on site j, while $K_j = e^{i\pi \sum_{i<j} n_i}$ is a string operator which simply accounts for the parity of the number of fermions

before site j (i.e., between site 1 and site $j-1$ of the chain), and thus multiplies the operator c_i by a phase-factor ± 1. Notice that, in order to apply the JWT, one needs to define an ordering of the various sites of the system. This can be naturally done in one dimension, but becomes less meaningful in higher dimensions, thus essentially limiting the usefulness of the transformation (11.22) to 1D systems.

Exercise 11.1 It is not difficult to verify that the string phase-factor K_j implies that the c_j fermions satisfy standard anti-commutation relations. Using the JWT defined in Eq. (11.22), show that indeed:

$$\{c_i, c_j^\dagger\} = \delta_{ij}, \quad \{c_i, c_j\} = \{c_i^\dagger, c_j^\dagger\} = 0. \tag{11.23}$$

To this purpose, you first first need to employ the mapping of Eq. (11.20), and then use the commutation relations of the Pauli matrices. It can be useful to preliminarily prove that $[\sigma_i^+, \sigma_j^-] = \delta_{ij}\,\sigma_j^z$ and $[\sigma_i^z, \sigma_j^\pm] = \pm 2\,\delta_{ij}\,\sigma_j^\pm$.

We conclude with a summary of a few useful expressions where the string K_j cancels out exactly, in view of the 1D geometry of the problem:

$$\begin{aligned}
a_j^\dagger a_j &= c_j^\dagger c_j, \\
a_j^\dagger a_{j+1}^\dagger &= c_j^\dagger (1-2n_j) c_{j+1}^\dagger = c_j^\dagger c_{j+1}^\dagger, \\
a_j^\dagger a_{j+1} &= c_j^\dagger (1-2n_j) c_{j+1} = c_j^\dagger c_{j+1}, \\
a_j a_{j+1} &= c_j (1-2n_j) c_{j+1} = c_j \big[1-2(1-c_j c_j^\dagger)\big] c_{j+1} = -c_j c_{j+1}, \\
a_j a_{j+1}^\dagger &= c_j (1-2n_j) c_{j+1}^\dagger = c_j \big[1-2(1-c_j c_j^\dagger)\big] c_{j+1}^\dagger = -c_j c_{j+1}^\dagger,
\end{aligned}$$

which can be readily obtained by noting that $K_j K_{j+1} = 1-2n_j$, since $(1-2n_i)(1-2n_i) = 1$, and terms with different site index commute. Using such relations, it is immediate to show that both terms of the Ising model transform in a simple way into local fermionic operators:

$$\sigma_j^z = 2a_j^\dagger a_j - 1 = 2n_j - 1, \tag{11.24}$$

$$\sigma_j^x \sigma_{j+1}^x = \big(a_j^\dagger a_{j+1}^\dagger + a_j^\dagger a_{j+1} + \text{H.c.}\big) = \big(c_j^\dagger c_{j+1}^\dagger + c_j^\dagger c_{j+1} + \text{H.c.}\big). \tag{11.25}$$

We can thus write the Hamiltonian of Eq. (11.21) in a fermionic language as

$$H = -J \sum_j \big(c_j^\dagger c_{j+1} + c_j^\dagger c_{j+1}^\dagger + \text{H.c.}\big) - h \sum_j (2n_j - 1). \tag{11.26}$$

A final important remark concerns the boundary conditions. One often assumes periodic boundary conditions (PBC) for spin operators, which in turn immediately implies the same boundary conditions for the hard-core bosons, that is, $a_L^\dagger a_{L+1} \equiv a_L^\dagger a_1$ (we identify site $L+1$ with site 1 in the chain). However, when rewriting such term using spinless fermions, we have:

$$a_L^\dagger a_1 = e^{i\pi \sum_{i=1}^{L-1} n_i} c_L^\dagger c_1 = -e^{i\pi \sum_{i=1}^{L} n_j} c_L^\dagger c_1 = -(-1)^{N_F} c_L^\dagger c_1, \tag{11.27}$$

where N_F denotes the total number of c_j-fermions that are present in the lattice. The second equality follows since, to the left of $c_L^\dagger$, one certainly has $n_L = 1$, and

thus we have: $-e^{i\pi n_L} = 1$. Analogously we find that $a_L^\dagger a_1^\dagger = -(-1)^{N_F} c_L^\dagger c_1^\dagger$. This shows that boundary conditions are affected by the fermionic parity $(-1)^{N_F}$: for an odd number N_F of fermions one gets PBC in the fermionic model, while for N_F even, anti-periodic boundary condition are found. Notice that, although the number of fermions is not conserved by the Hamiltonian (11.26), its parity is conserved and $(-1)^{N_F}$ is a constant of motion, with value ± 1. Summarizing, in fermionic language, for an even number of fermions we have anti-periodic boundary conditions (that is, the L-th bond has an opposite sign with respect to the other ones: $c_{L+1} = -c_1$). On the opposite, for an odd number of fermions periodic boundary conditions are required (all the bonds have the same sign: $c_{L+1} = c_1$).

11.3.2 *Diagonalization of the Ising chain*

Since the Hamiltonian of Eq. (11.26) conserves the fermion parity, both the even (+) and the odd (−) sector of the fermionic Hilbert space have to be considered when diagonalizing the model. Let us denote with $H^\pm$ the two even/odd Hamiltonian subspace restrictions, such that $H = H^+ + H^-$. Due to the translational invariance of the model (11.19), it is very helpful to switch to momentum space, and define a Fourier transform of the fermionic operators according to:

$$c_j = \frac{1}{\sqrt{L}} \sum_k d_k e^{i\frac{2\pi}{L}kj}, \qquad j = 1, \ldots, L. \tag{11.28}$$

In order to properly choose the possible values of the momenta k, we shall distinguish various cases, according to the parities of L and N_F. Recall that, according to the parity of N_F, the following fermionic boundary conditions are required: $c_{L+1} = \pm c_1$, where the plus sign is for N_F odd, while the minus sign is for N_F even. This is equivalent to asking that $e^{i\frac{2\pi}{L}kL} = \pm 1$. Without loss of generality, let us now redefine the labelling of sites using the following practical convention:

$$j = \begin{cases} -\frac{L-1}{2}, -\frac{L-3}{2}, -\frac{L-5}{2}, \ldots, +\frac{L-1}{2} & (L \text{ odd}), \\ -\frac{L}{2}+1, -\frac{L}{2}+2, -\frac{L}{2}+3, \ldots, +\frac{L}{2} & (L \text{ even}). \end{cases} \tag{11.29}$$

Therefore with this labelling, we can use the following momenta (in units of $2\pi/L$):

$$k = \begin{cases} -\frac{L-1}{2}, -\frac{L-3}{2}, -\frac{L-5}{2}, \ldots, +\frac{L-1}{2} & (N_F + L \text{ even}), \\ -\frac{L}{2}+1, -\frac{L}{2}+2, -\frac{L}{2}+3, \ldots, +\frac{L}{2} & (N_F + L \text{ odd}). \end{cases} \tag{11.30}$$

Exercise 11.2 Prove the consistency of our choice (11.30) with the boundary conditions for fermions.

Using the transformation (11.28), it is now possible to rewrite the two $H^\pm$ Hamiltonian sectors in momentum space (with the appropriate choice of the k-

vectors), according to:

$$H^{\pm} = -\frac{J}{L}\sum_j \sum_{k,k'} \Big\{ d_k^\dagger d_{k'} \Big(e^{i\frac{2\pi}{L}\left[-kj+k'(j+1)\right]} + e^{i\frac{2\pi}{L}\left[-k(j+1)+k'j\right]} + \frac{2h}{J} e^{i\frac{2\pi}{L}\left[-kj+k'j\right]} \Big) + d_k^\dagger d_{k'}^\dagger e^{i\frac{2\pi}{L}\left[-kj-k'(j+1)\right]} + d_k d_{k'} e^{i\frac{2\pi}{L}\left[k(j+1)+k'j\right]} - \frac{h}{J}\delta_{k,k'} \Big\}$$
$$= -J\sum_k \Big\{ d_k^\dagger d_k \Big(e^{i\frac{2\pi}{L}k} + e^{-i\frac{2\pi}{L}k} + \frac{2h}{J} \Big) + e^{i\frac{2\pi}{L}k} \big(d_k^\dagger d_{-k}^\dagger + d_k d_{-k} \big) - \frac{h}{J} \Big\}, \quad (11.31)$$

where we used the completeness relation $\frac{1}{L}\sum_j e^{i\frac{2\pi}{L}kj} = \delta_{k,0}$. Notice the coupling of $-k$ with k, with the exceptions of momenta 0 and π for the cases where they appear (i.e., $k = 0$ and $k = L/2$ in units of $2\pi/L$), which do not have a separate $-k$ partner. It is thus possible to group together terms with opposite momenta, such that the Hamiltonian is eventually decoupled into a sum of independent terms acting in the four-dimensional Hilbert spaces generated by k and $-k$:

$$H^+ = \sum_{k>0} H_k^+, \qquad H^- = \sum_{k>0} H_k^- + H_0 + H_{L/2} \qquad (L \text{ even}) \quad (11.32)$$

$$H^+ = \sum_{k>0} H_k^+ + H_{L/2}, \qquad H^- = \sum_{k>0} H_k^- + H_0 \qquad (L \text{ odd}). \quad (11.33)$$

Here we have singled out the unpaired contributions $H_0 = -2(J+h)n_0 + h$ and $H_{L/2} = 2(J-h)n_{L/2} + h$ (corresponding to $k = 0$ and $k = L/2$), and defined

$$H_k^{\pm} = -2\left[J\cos\left(\tfrac{2\pi k}{L}\right) + h\right]\left(d_k^\dagger d_k - d_{-k} d_{-k}^\dagger\right) - 2iJ\sin\left(\tfrac{2\pi k}{L}\right)\left(d_k^\dagger d_{-k}^\dagger - d_{-k} d_k\right), \quad (11.34)$$

exploiting the anti-commutation relations for the fermions, and the fact that the cosine is an even function, while $d_k^\dagger d_{-k}^\dagger - d_{-k} d_k$ is odd with respect to $k \to -k$. Now we introduce the two variables

$$f_k = -2\left[J\cos\left(\tfrac{2\pi k}{L}\right) + h\right], \quad g_k = 2J\sin\left(\tfrac{2\pi k}{L}\right). \quad (11.35)$$

In this way, the expression for $H_k^{\pm}$ can be recast in a compact form using the so-called Nambu formalism, with the fermionic two-component spinor $\Psi_k^\dagger = \left[d_k^\dagger,\ d_{-k}\right]$:

$$H_k = \left[d_k^\dagger\ \ d_{-k}\right] \begin{bmatrix} f_k & -ig_k \\ ig_k & -f_k \end{bmatrix} \begin{bmatrix} d_k \\ d_{-k}^\dagger \end{bmatrix} \equiv \Psi_k^\dagger \mathbb{H}_k \Psi_k, \quad (11.36)$$

where we omitted the apex $^{\pm}$, and defined $\mathbb{H}_k = f_k\sigma_z + g_k\sigma_y$.

Bogoliubov rotation

We will now focus on the diagonalization of the 2×2 Hamiltonian in Eq. (11.36), since the unpaired terms H_0 and $H_{L/2}$ appearing in Eqs. (11.32)-(11.33) are already in a diagonal form. The matrix $\mathbb{H}_k$ can be readily diagonalized by taking a rotation $R_x(\theta_k)$ of an angle $\theta_k = \arctan(g_k/f_k)$ around the x axis, that is, we introduce the unitary operator

$$U_k \equiv R_x(\theta_k) = \exp\left(i\tfrac{\theta_k}{2}\sigma^x\right) = \cos\left(\tfrac{\theta_k}{2}\right)\mathbb{I} + i\sin\left(\tfrac{\theta_k}{2}\right)\sigma^x. \quad (11.37)$$

The corresponding eigenvalues are given by:

$$\varepsilon_k^{\pm} = \pm\varepsilon_k, \quad \text{with } \varepsilon_k = \sqrt{f_k^2 + g_k^2} = 2J\sqrt{1 + \tfrac{h^2}{J^2} + \tfrac{2h}{J}\cos\left(\tfrac{2\pi k}{L}\right)}, \tag{11.38}$$

while the change-of-basis matrix U_k applied to the Ψ_k fermions defines the new operators $\Phi_k = U_k^\dagger \Psi_k$, which diagonalize the problem:

$$\Phi_k \equiv \begin{bmatrix} b_k \\ b_{-k}^\dagger \end{bmatrix} = \begin{bmatrix} \cos(\theta_k/2) & -i\sin(\theta_k/2) \\ -i\sin(\theta_k/2) & \cos(\theta_k/2) \end{bmatrix} \begin{bmatrix} d_k \\ d_{-k}^\dagger \end{bmatrix}. \tag{11.39}$$

If we now define $u_k = \cos(\theta_k/2) = f_k/\varepsilon_k$ and $v_k = \sin(\theta_k/2) = g_k/\varepsilon_k$, such that $u_{-k} = u_k$, $v_{-k} = -v_k$, and $u_k^2 + v_k^2 = 1$, Eq. (11.39) can be rewritten as:

$$\begin{cases} b_k &= u_k d_k - i v_k d_{-k}^\dagger \\ b_{-k}^\dagger &= -i v_k d_k + u_k d_{-k}^\dagger \end{cases}. \tag{11.40}$$

It is then immediate to verify that the b_k operators obey anti-commutation relations:

$$\{b_k, b_k^\dagger\} = \{u_k d_k - i v_k d_{-k}^\dagger, i v_k d_{-k} + u_k d_k^\dagger\} = u_k^2 \{d_k, d_k^\dagger\} + v_k^2 \{d_{-k}^\dagger, d_{-k}\} = 1, \tag{11.41}$$

and thus correspond to fermionic quasiparticles. Summarizing, we can write the Hamiltonian H_k of Eq. (11.36) in a diagonal form as

$$H_k = \Psi_k^\dagger U_k \big(U_k^\dagger \mathbb{H}_k U_k\big) U_k^\dagger \Psi_k = \Phi_k^\dagger \begin{bmatrix} \varepsilon_k & 0 \\ 0 & -\varepsilon_k \end{bmatrix} \Phi_k = \varepsilon_k \big(b_k^\dagger b_k + b_{-k}^\dagger b_{-k} - 1\big). \tag{11.42}$$

The procedure outlined here to diagonalize the fermionic Hamiltonian (11.36) in momentum space is called *Bogoliubov rotation*, while the operators b_k over which the Hamiltonian becomes diagonal are associated to the Bogoliubov *quasiparticles* of the Ising model.

Exercise 11.3 Show that, using the same approach described above, it is possible to diagonalize a generic fermionic quadratic Hamiltonian of the type:

$$H = \sum_{i,j} c_i^\dagger A_{i,j} c_j + \tfrac{1}{2} \sum_{i,j} \Big\{ c_i^\dagger B_{i,j} c_j^\dagger + \text{H.c.} \Big\}, \tag{11.43}$$

where A needs to be a Hermitian matrix, due to the hermiticity of H, and B needs to be a skew-symmetric matrix, due to the anti-commutation rules among the c_j fermions. This construction generalizes the Bogoliubov rotation (11.39) for the $\{k, -k\}$ momentum space, to the $2L$ dimensional real space of the fermionic $\{c_j\}_{j=1,\ldots,L}$ and $\{c_j^\dagger\}_{j=1,\ldots,L}$ operators.

Ground state

The expression (11.42) allows to conclude that, neglecting momenta 0 and π (when they appear), the ground state of the Hamiltonian must be the state $|\psi_0\rangle$ which annihilates the b_k quasiparticles for all k, also called the *Bogoliubov vacuum*:

$$b_k |\psi_0\rangle = 0, \quad \forall\, k. \tag{11.44}$$

Moreover, the energy dispersion relation of Eq. (11.38) tells us that the low-energy excitations (i.e., those minimizing ε_k) are quasiparticles with $k \to L/2$ (corresponding to a momentum π, in units of $2\pi/L$), which behave as:

$$\lim_{\tilde{k}\to 0} \varepsilon_{\tilde{k}} = \begin{cases} 2|h-J| + \frac{4\pi^2 Jh}{|h-J|L^2}\tilde{k}^2 & \text{if } h \neq J, \\ \frac{4\pi}{L}\tilde{k} & \text{if } h = J, \end{cases} \tag{11.45}$$

with $\tilde{k} = k - L/2$. Therefore they exhibit a quadratic dispersion for $h \neq J$, and a linear dispersion for $h = J$. This also means that the energy gap between the ground state and the first excited state $\Delta_E^{(0)} = 2|h - J|$ is always finite, except at $h = J$ which is also called a gapless point. As we shall see later, the point $h_c = J$ corresponds to a critical value for which the thermodynamic properties of the system exhibit a dramatic change [4]. This is a so-called *quantum critical point*.

All the conclusions drawn above hold for systems which are so large that the discretization of the momenta k makes the two uncoupled values 0 and $L/2$, as well as any detail on the choices of Eqs. (11.29)-(11.30), completely irrelevant. This is the case when the thermodynamic limit $L \to \infty$ is approached. However, for finite systems, one should pay attention to the fact that, in principle, there are two competing ground states, coming from the N_F-even and from the N_F-odd parity sector. Moreover we recall that periodic boundary conditions have to be adopted with an odd number of fermions (thus resulting in the Hamiltonian H^-), and anti-periodic boundary conditions hold with an even number of fermions (thus resulting in the Hamiltonian H^+).

Specifically, in order to analyze the energies of the two ground states, we need to look at the specific form of the Hamiltonian, Eqs. (11.32) and (11.33), keeping in mind that, for a chain of length L, the vacuum of quasiparticles has always a parity $(-1)^L$. Let us also recall that the excitation energy for adding a $k = 0$ quasiparticle is $\varepsilon_0 = -2(J + h)$ and that for adding a $k = L/2$ quasiparticle is $\varepsilon_{L/2} = 2(J - h)$. Therefore, for $h > J$ both ε_0 and $\varepsilon_{L/2}$ are negative (and thus the creation of unpaired quasiparticles is favoured), for $h < -J$ both ε_0 and $\varepsilon_{L/2}$ are positive (and thus the creation of unpaired quasiparticles is unfavoured), for $|h| < J$ one of the two unpaired quasiparticles has positive energy, the other has negative energy. In conclusion we have various situations.

- For $h < -J$ only the vacuum state with an even number N_F of fermions is permitted. The other vacuum does not match the required boundary conditions, therefore one particle with a positive and finite energy has to be added, thus lifting it to an excited state.
- For $h > J$ again only one vacuum state is permitted: this corresponds to N_F even if L is even, and to N_F odd if L is odd.
- For $|h| < J$ both two vacua, with N_F even and with N_F odd are permitted. This ends up into a quasi-degeneracy in the ground state, that becomes exact in

[4] An analogous behaviour occurs at $h = -J$. It is however important to stress that, for $h < 0$, the spectrum is reversed and thus one should look at excitations close to $k = 0$.

the thermodynamic limit. We will come back to this point later in Sec. 11.3.5.

Duality mapping

The peculiarity of the $h = \pm J$ points is also signaled by the fact that it is possible to perform a canonical transformation of the spins $\sigma_j^\alpha \to \tau_j^\alpha$ that preserves the structure of the Hamiltonian (11.19), and inverts the roles of the coupling constants J and h. Namely, this is defined by

$$\tau_j^x = \prod_{k<j} \sigma_k^z; \qquad \tau_j^z = \sigma_j^x \sigma_{j+1}^x, \tag{11.46}$$

such that the Ising model in these new variables becomes

$$H_\tau = -J \sum_j \tau_j^z - h \sum_j \tau_j^x \tau_{j+1}^x. \tag{11.47}$$

Setting $J = 1$ for simplicity, we find that $H_\sigma(h) \longleftrightarrow h \times H_\tau(h^{-1})$, where we only expressed the dependence of the model on the field, and H_σ denotes the original Hamiltonian of Eq. (11.19). The symbol $\longleftrightarrow$ indicates the equivalence of two Hamiltonians, up to a canonical transformation. This self-duality property guarantees an identical spectral structure of the system in correspondence of fields with strength h and $1/h$, thus imposing the existence of a critical point at $h = J$ (and a symmetric one at $h = -J$), if we assume that the latter is unique.

Correlation functions

We are now in the position to discuss how the integrability of the model can be exploited in order to extrapolate physical quantities, such as spin magnetizations or correlation functions. To this purpose, for a chain with L sites (we will take L odd) it is first convenient to introduce the following $2L$ operators γ_j, with $j = -L, -L+1, \ldots, L-1$:

$$\gamma_{2j-1} = \Big(\prod_{m<j} \sigma_m^z \Big) \sigma_j^x, \qquad \gamma_{2j} = \Big(\prod_{m<j} \sigma_m^z \Big) \sigma_j^y. \tag{11.48}$$

Notice that the string $\prod_{m<j} \sigma_m^z$ corresponds exactly to the one in front of Eq. (11.22), in the standard JWT. Now, using the fact that $\sigma_j^x = \sigma_j^+ + \sigma_j^-$ and $\sigma_j^y = -i(\sigma_j^+ - \sigma_j^-)$, we obtain the following peculiar property:

$$\gamma_{2j-1} = c_j^\dagger + c_j, \qquad \gamma_{2j} = -i(c_j^\dagger - c_j), \tag{11.49}$$

thus implying that the operators defined in (11.48) are Hermitian: $\gamma_j^\dagger = \gamma_j$. Any particle respecting this rule is called a *Majorana fermion*.

We are now going to show that any possible spin-correlation function of the Ising model can be obtained by knowing the $2L \times 2L$ correlation matrix Γ_L of the above Majorana operators, whose matrix elements are defined by:

$$\big[\Gamma_L\big]_{m,n} = \langle \gamma_m \gamma_n \rangle, \qquad m, n = -L, \ldots, L-1. \tag{11.50}$$

Hereafter, unless specified, the averages of any obsesrvable $\mathcal{O}$ have to be intended on the ground state: $\langle \mathcal{O} \rangle = \langle \psi_0 | \mathcal{O} | \psi_0 \rangle$. The ground-state expectation values $\langle \gamma_m \gamma_n \rangle$,

entering the various matrix elements of Γ_L, are computed by applying a sequence of recursive transformations which map γ_j-Majorana operators into c_j-fermions, then into d_k-fermions, and finally into the Bogoliubov b_k-quasiparticles that diagonalize the model. Putting them all together, we get

$$\begin{bmatrix} \gamma_{2j-1} \\ \gamma_{2j} \end{bmatrix} = \frac{1}{\sqrt{L}} \sum_k e^{i\frac{2\pi}{L}kj} \begin{bmatrix} 1 & 1 \\ i & -i \end{bmatrix} \begin{bmatrix} u_k & iv_k \\ iv_k & u_k \end{bmatrix} \begin{bmatrix} b_k \\ b^\dagger_{-k} \end{bmatrix}. \tag{11.51}$$

As a matter of fact, from Eq. (11.44) we know that the ground state is defined as the one that is annihilated by all such b_k particles. Therefore we have [5]:

$$\langle b_k\, b^\dagger_{k'}\rangle = \delta_{kk'}; \quad \langle b_k\, b_{k'}\rangle = \langle b^\dagger_k\, b^\dagger_{k'}\rangle = \langle b^\dagger_k\, b_{k'}\rangle = 0. \tag{11.52}$$

Combining this with the relations (11.51), one can finally arrive to the following:

$$\big[\Gamma_L\big]_{mn} = \delta_{mn} + i\Lambda_{mn}, \quad \text{with} \quad \Lambda_{mn} = \begin{bmatrix} \Pi_0 & \Pi_1 & \cdots & \Pi_{L-1} \\ -\Pi_1 & \Pi_0 & \cdots & \Pi_{L-2} \\ \vdots & \vdots & & \vdots \\ -\Pi_{L-1} & -\Pi_{L-2} & \cdots & \Pi_0 \end{bmatrix}, \tag{11.53}$$

where Λ is a skew-symmetric matrix with sub-blocks

$$\Pi_j = \begin{bmatrix} 0 & g(j) \\ -g(-j) & 0 \end{bmatrix}, \qquad g(j) = \frac{1}{L} \sum_k e^{i\frac{2\pi}{L}kj}\, e^{i\theta_k/2}, \tag{11.54}$$

and θ_k is the Bogoliubov angle defined above. In the thermodynamic limit we can write explicitly:

$$g(j) = \frac{1}{2\pi} \int_0^{2\pi} d\phi\, e^{i\phi j}\, \frac{J\cos\phi + h - iJ\sin\phi}{|J\cos\phi + h - iJ\sin\phi|}. \tag{11.55}$$

Now suppose that we want to calculate a two-point correlation function of the form $\langle \sigma^\alpha_j\, \sigma^\beta_l\rangle$. First we have to express the Pauli matrices in terms of the Majorana fermions γ_j, using their definition (11.48):

$$\sigma^x_j = \Big(\prod_{m<j} \sigma^z_m\Big)\gamma_{2j-1}, \quad \sigma^y_j = \Big(\prod_{m<j} \sigma^z_m\Big)\gamma_{2j}, \quad i\sigma^z_j = \sigma^x_j\sigma^y_j = \gamma_{2j-1}\gamma_{2j}. \tag{11.56}$$

From this it is clear that σ^z correlators can be calculated straightforwardly, since they do not involve JW strings. On the other hand, correlators involving for example $\langle \sigma^x_j\, \sigma^x_l\rangle$ are expressed as an expectation value of a string of Majorana fermions:

$$\langle \sigma^x_j\, \sigma^x_l\rangle = \langle \gamma_{2j}\, \gamma_{2j+1} \cdots \gamma_{2l-1}\rangle, \tag{11.57}$$

where we used the fact that $\gamma_{2j-1}\,\gamma_{2j-1} = (c^\dagger_j + c_j)(c^\dagger_j + c_j) = 1$. These contractions can be drastically simplified by applying Wick's theorem to expectation values taken with respect to the ground (or the thermal) state of free-Fermi theory:

$$\langle \gamma_{2j}\, \gamma_{2j+1} \ldots \gamma_{2l-1}\rangle = \sum_{\text{all pairings}} (-1)^P \prod_{\text{all pairs}} (\text{contraction of all pairs}), \tag{11.58}$$

[5] All the calculations presented here can be generalized to fermionic thermal states, observing that the relations (11.52) transform into: $\langle b^\dagger_k b_{k'}\rangle_\beta = \delta_{kk'}/\big[1 + \exp(\beta\varepsilon_k)\big] = \delta_{kk'} - \langle b_k b^\dagger_{k'}\rangle_\beta$, and $\langle b^\dagger_k b^\dagger_{k'}\rangle_\beta = \langle b_k b_{k'}\rangle_\beta = 0$, where we used the Fermi-Dirac statistics and $\beta = 1/(k_B T)$.

where $(-1)^P$ is the parity of the permutation that takes the indexes $_{2j,2j+1,\ldots,2l-1}$ into any sequence defining a string of operators to be contracted in pairs. The sum over all the pairings of the product of the pair contractions coincides with the square root of the determinant (i.e., the Pfaffian) of the $(2l-2j)\times(2l-2j)$ reduced matrix $\Gamma^{(R)}_{l-j}$, obtained as a diagonal sub-block of the full correlation matrix Γ_L. This method is applicable to any spin-correlation function, which can be always taken as the expectation value of a string of Majorana fermions, as in Eq. (11.58).

A physically relevant result in this respect is the magnetization M^x along the coupling direction, obtainable as the long-distance limit of the two-point correlation: $\lim_{n\to\infty}\langle\sigma^x_j\sigma^x_{j+n}\rangle = (M^x)^2$, which can be calculated to give

$$M_x \,=\, \langle\sigma_x\rangle \,=\, \begin{cases} \left(1-\frac{h^2}{J^2}\right)^{1/8} & \text{if } |h| \,<\, J, \\ 0 & \text{if } |h| \,\geq\, J, \end{cases} \tag{11.59}$$

where we omitted the irrelevant site index j, for a translationally invariant system. This shows once more that $h_c = \pm 1$ is a special point, separating a region where the ground state of the system is unpolarized along the x axis ($|h| > |h_c|$), from another one where the x-axis magnetization acquires a finite value ($|h| < |h_c|$). More precisely, h_c denotes the onset of a zero-temperature *quantum phase transition*, where, as a consequence of a variation of the field strength h, the ground state undergoes drastic modifications: it changes from an x-paramagnet, where $\langle\sigma_x\rangle = 0$, to an x-ferromagnet, where $\langle\sigma_x\rangle \neq 0$. In passing we mention that the phenomenology outlined here is closely related to the finite-temperature phase transition in the classical Ising model above two dimensions (in the sense that the critical properties of the two phase transitions are the same), provided the parameter h is substituted by the temperature T and "quantum" fluctuations are replaced by "thermal" fluctuations. The interested reader can find a detailed discussion, for example, in Sachdev (2011).

11.3.3 *Two-spin concurrence*

A quantum phase transition may also reveal in a dramatic change of the ground-state entanglement pattern. Following the works by Osterloh *et al.* (2002) and Osborne and Nielsen (2002), we validate this statement by discussing the behaviour of the pairwise entanglement between any two spins i and j in the Ising model, when the transverse field h is varied. As shown in Sec. 6.7.1, it is possible to provide an analytic expression for the entanglement of formation of two qubits as a monotone of the so-called concurrence. Here we focus precisely on the concurrence C_d, where $d = |i-j|$ denotes the distance between any two spin-1/2 particles.

It can be proven that, for any spin-chain model exhibiting the parity symmetry $\left[H, \otimes_j \sigma^z_j\right] = 0$, all the components of the wave function have an even (or odd) number of flipped spins. Under such restriction, the most general reduced density matrix of two arbitrary spins assumes a so-called X-shape, in which the only non-